The Origin of Outflows in Evolved Stars
Proceedings IAU Symposium No. 366, 2022
L. Decin, A. Zijlstra & C. Gielen, eds.
doi:10.1017/S1743921322000205

Lessons from the ionised and molecular mass of post-CE PNe

Miguel Santander-García[1], David Jones[2,3], Javier Alcolea[1], Valentín Bujarrabal[4] and Roger Wesson[5]

[1]Observatorio Astronómico Nacional (OAN-IGN), Alfonso XII, 3, 28014, Madrid, Spain
email: m.santander@oan.es

[2]Instituto de Astrofísica de Canarias, 38205, La Laguna, Spain

[3]Departamento de Astrofísica, Universidad de La Laguna, 38206, La Laguna, Spain

[4]Observatorio Astronómico Nacional (OAN-IGN), Apdo. 112, 28803, Alcalá de Henares, Spain

[5]Department of Physics and Astronomy, University College London, Gower St, London, UK

Abstract. Close binary evolution is widely invoked to explain the formation of axisymmetric planetary nebulae, after a brief common envelope phase. The evolution of the primary would be interrupted abruptly, its still quite massive envelope being fully ejected to form the PN, which should be more massive than a planetary nebula coming from the same star, were it single. We test this hypothesis by investigating the ionised and molecular masses of a sample consisting of 21 post-common-envelope planetary nebulae, roughly one fifth of their known total population, and comparing them to a large sample of regular planetary nebulae (not known to host close-binaries). We find that post-common-envelope planetary nebulae arising from single-degenerate systems are, on average, neither more nor less massive than regular planetary nebulae, whereas post-common-envelope planetary nebulae arising from double-degenerate systems are considerably more massive, and show substantially larger linear momenta and kinetic energy than the rest. Reconstruction of the common envelope of four objects further suggests that the mass of single-degenerate nebulae actually amounts to a very small fraction of the envelope of their progenitor stars. This leads to the uncomfortable question of where the rest of the envelope is, raising serious doubts on our understanding of these intriguing objects.

Keywords. planetary nebulae: general, planetary nebulae: individual: NGC 6778, circumstellar matter, binaries: close, Stars: mass-loss, Stars: winds, outflows

1. Introduction

Planetary nebulae (PNe) display beautiful, complex morphologies often showing high degrees of symmetry, mostly elliptical or bipolar. Among the mechanisms usually invoked to explain their intriguing shaping (Balick & Frank, 2002), angular momentum transfer from a companion is currently considered a key ingredient (Jones & Boffin 2017; Decin *et al.* 2020). In the case of a sufficiently close companion, the system undergoes a common envelope (CE) event when the primary star evolves along the giant branch(es), expanding before eventually overflowing its Roche lobe and engulfing its companion (Paczynski 1976). In this very brief stage (∼1 year), the orbit of the secondary star quickly shrinks due to drag forces, providing angular momentum for the system to eject the CE, which we will observe as a PN.

From an observational point of view, the number of confirmed post-CE PNe has been quickly growing over the last decades, amounting to around 100 objects so far†. On theoretical grounds, nevertheless, the mechanism of CE ejection remains elusive, with most hydrodynamic models unable to gravitationally unbind the whole envelope without recurring to additional energy reservoirs such as recombination energy from the ionised regions (e.g. Ricker & Taam 2012; Jones 2020; Ohlmann *et al.* 2016; Ivanova 2018; Chamandy *et al.* 2020). To sum up, simulations collectively show that the CE has a major role in shaping PNe, but we are far from fully understanding the physics behind the death of a significant fraction of stars in the Universe.

Carefully estimating the actual mass of post-CE PNe could help towards a better understanding of the physics of CE ejection. In this respect, it can be helpful to establish comparisons between these objects and the general population of PNe, encompassing nebulae arising not only from close binaries but also from single stars and longer period binary stars that did not experience a CE. The only existing previous work covering this topic studied the ionised mass of a sample of post-CE PNe, suggesting these objects are slightly less massive, on average, than the general population of PNe (Frew & Parker 2007).

In this work we systematically analyse the mass of post-CE PNe, extending it to cover molecular masses as well as ionised ones, on a sample comprising 21 post-CE PNe (roughly 1/5th of the total known population of these objects), and putting it into context by comparing it to a larger sample of 97 'regular' PNe (nebulae not known to arise from close-binary systems). This proceeding summarises the main results of our study. Please consult the main publication for additional details, information on the methods followed and general discussion on the mass of post-CE PNe (Santander-García *et al.* 2022).

2. Sample and Observations

We used the IRAM 30m radiotelescope to carry out mm-wavelength observations in order to probe the molecular content of an initial sample of nine post-CE PNe of the northern sky which were previously unobserved in ^{12}CO and ^{13}CO J=1−0 and J=2−1. Only one of them, NGC 6778, was detected, and its molecular emission profiles were indicative of the presence of a thin ring-like structure along the equator of the nebula, located outwards from the equatorial ionised, broken ring visible in optical images (Guerrero & Miranda 2012). See Santander-García *et al.* (2022) for a spatiokinematical model of this structure including radiative-transfer of CO species.

The sample was later extended to 21 post-CE PNe, including objects with molecular observations published in the literature (Huggins & Healy 1989; Huggins *et al.* 1996, 2005; Guzman-Ramirez 2018). Note that only 3 of these 21 objects, NGC 6778, NGC 2346, and NGC 7293, show molecular emission at all, hence the molecular masses computed below are upper limits in most cases.

In addition to the molecular data, we also gathered dereddenned Hα fluxes and optical sizes from Frew *et al.* (2016), as well as literature-based values of the densities and electronic temperatures of every object in the sample.

3. The mass of post-CE PNe

We computed the ionised and molecular masses of the whole sample of post-CE PNe in a systematic way. We here describe the analyses performed, present our results on the masses, and compare them to the masses of a large sample of 'regular' PNe estimated in the same way.

† See updated list with references to discovery papers in `http://www.drdjones.net/bcspn/`

https://doi.org/10.1017/S1743921322000205 Published online by Cambridge University Press

3.1. *Ionised masses*

The total ionised masses of the PNe were calculated as:

$$M_{\rm ion} = \frac{4\ \pi\ D^2\ F({\rm H}\beta)\ m_p}{h\nu_{{\rm H}\beta}\ n_e\ \alpha^{\rm eff}_{{\rm H}\beta}}, \tag{3.1}$$

where D is the distance, $F(\mathrm{H}\beta)$ is the dereddened, spatially integrated Hβ flux, m_p is the mass of the proton, $h\nu_{\mathrm{H}\beta}$ is the energy of an Hβ photon, n_e is the electron density, and $\alpha^{\rm eff}_{\mathrm{H}\beta}$ is the effective recombination coefficient of Hβ (Corradi *et al.* 2015).

For the results to be as standardised as possible, we only utilised Hβ fluxes derived from the dereddened Hα surface brightness tabulated by Frew *et al.* (2016), integrated over the ellipse defined by the minor and major axes tabulated in the same work. With respect to electron temperatures, we used T[O III] determinations when possible, and assumed T_e=10 000 K in those objects where no determination was available. Similarly, we used [S II] line doublet determinations of the electron densities (except for NGC 246, where only an estimate based on [O II] was available). Note that, if part of the nebulae consist of dense condensations above the density traced by [S II], the resulting ionised masses would in principle be lower (adding to the problem outlined below). As for distances, we prioritised GAIA eDR3 determinations by Gaia *et al.* (2020), and their associated errors were $< 33\%$. In the absence of these, we used distances by Frew *et al.* (2016).

3.2. *Molecular masses*

We computed the molecular mass for the three objects in our sample which show molecular emission, as well as conservative (3-σ) upper limits to the molecular mass of the rest of the objects in the sample. We assume that: *(i)* the CO level populations are in local thermodynamic equilibrium (LTE), and are characterised by an excitation temperature $T_{\rm ex}$; *(ii)* the CO abundance X relative to molecular hydrogen is constant throughout the nebula; and *(iii)* the selected CO transition is optically thin. Under these conditions, the molecular mass $M_{\rm mol}$ of the nebula is:

$$M_{\rm mol} = \frac{4\ \pi\ m_{\rm H_2}\ D^2}{A_{\rm ul}\ X\ h\ \nu\ g_u}\ e^{\frac{h\nu}{kT_{\rm ex}}}\ Z(T_{\rm ex})\ f_{\rm He}\ S_\nu, \tag{3.2}$$

where $m_{\rm H_2}$ is the mass of the hydrogen molecule, h and k are the Planck and Boltzmann constants, ν is the frequency of the transition, $A_{\rm ul}$ its Einstein coefficient, g_u the degeneracy of its upper state, Z the partition function, D the distance to the nebula, $\mathrm{f_{He}}$ the correction factor to account for helium abundance (assumed to be He/H=0.1 and thus resulting in $\mathrm{f_{He}}$=1.2, because we also assume the majority of particles to be of molecular hydrogen), and S_ν the flux density:

$$S_\nu = \frac{2\ k\ \nu^2\ F}{c^2}, \tag{3.3}$$

where c is the speed of light in vacuum, and F the total flux of the nebula in the given transition, integrated both spatially and spectrally. We assumed an excitation temperature of $T_{\rm ex}$=50 K, and a CO abundance X=2×10^{-4} for every object in our calculations, and used primarily the ^{12}CO J=2−1 transition, more ubiquous and better detected in the literature. In order to overcome the clear limitation that this transition (as well as the ^{12}CO J=3−2 one) is usually not optically thin, we introduce a correction factor for the underestimated masses resulting from J=2−1 (and J=3−2) transitions in order to match masses found via the J=1−0 transition in a sample of PNe in which both transitions are available in the literature (Huggins & Healy 1989; Huggins *et al.* 1996, 2005; Guzman-Ramirez 2018). These resulted in a factor 3.65 to calculations using ^{12}CO J=2−1 and a factor 5.0 for those using ^{12}CO J=3−2. We recall that the best correction

https://doi.org/10.1017/S1743921322000205 Published online by Cambridge University Press

Table 1. Computed ionised and molecular masses of the post-CE sample.

PN G	Common name	D (kpc)	$M_{\rm ion}$ ($M_\odot$)	$M_{\rm mol}$ ($M_\odot$)
		Single-Degenerate post-CE PNe		
G034.5-06.7	NGC 6778	2.79±0.79	$0.19^{+0.14}_{-0.10}$	0.02±0.02
G036.1-57.1	NGC 7293	0.200±0.002	$0.09^{+0.13}_{-0.05}$	0.3±0.2
G053.8-03.0	Abell 63	2.703±0.219	$0.012^{+0.04}_{-0.009}$	<0.006
G054.2-03.4	Necklace	4.6±1.1	$0.009^{+0.017}_{-0.006}$	<0.007
G068.1+11.1	ETHOS 1	4.2±0.0	$0.008^{+0.3}_{-0.008}$	<0.007
G086.9-03.4	Ou 5	5.0±1.0	$0.18^{+0.4}_{-0.12}$	<0.012
G118.8-74.7	NGC 246	0.556±0.025	$0.07^{+0.12}_{-0.05}$	<0.02
G208.5+33.2	Abell 30	2.222±0.148	$0.015^{+0.02}_{-0.009}$	<0.20
G215.6+03.6	NGC 2346	1.389±0.039	$0.09^{+0.09}_{-0.04}$	0.7±0.5
G221.8-04.2	PM 1-23	5.2±2.0	$0.015^{+1.2}_{-0.014}$	<0.17
G307.5-04.9	MyCn 18	4.000±1.280	$0.07^{+0.10}_{-0.04}$	<0.06
G338.1-08.3	NGC 6326	5.000±1.500	$0.6^{+0.5}_{-0.3}$	<0.06
G338.8+05.6	Hen 2-155	4.348±1.323	$0.3^{+0.2}_{-0.14}$	<0.10
G342.5-14.3	Sp 3	$2.22^{+0.61}_{-0.48}$	$0.09^{+0.08}_{-0.04}$	<0.06
G349.3-04.2	Lo 16	1.818±0.132	$0.4^{+0.7}_{-0.3}$	<0.013
		Double-Degenerate post-CE PNe		
G009.6+10.5	Abell 41	4.89±1.4	$0.16^{+0.15}_{-0.09}$	<0.011
G049.4+02.4	Hen 2-428	4.545±1.446	$0.7^{+0.8}_{-0.4}$	<0.010
G058.6-03.6	V458 Vul	12.5±2.0	$0.11^{+0.19}_{-0.07}$	<0.08
G197.8+17.3	NGC 2392	1.818±0.165	$0.4^{+0.4}_{-0.19}$	<0.09
G290.5+07.9	Fg 1	2.564±0.197	$0.4^{+0.2}_{-0.15}$	<0.09
G307.2-03.4	NGC 5189	1.471±0.043	$0.11^{+0.03}_{-0.03}$	<0.09

factor will vary from nebula to nebula, and that this method is meant to be statistically meaningful in order to allow for comparisons with the ionised mass of these objects, and among subclasses of post-CE PNe.

3.3. *Results*

The resulting masses of the studied post-CE PNe are displayed in Table 1. Interestingly, a trend arises when we divide the sample in the categories of single-degenerate (SD) and double-degenerate (DD) systems, according to one or both components of the binary pair being a post-AGB star: PNe hosting DD systems are considerably more massive, on average, than their SD counterparts. Thus, the geometric mean of the ionised+molecular mass for the SD sample is 0.15 $M_\odot$, with a geometric standard deviation (GSD) factor of 3.4, whereas for the DD sample the geometric mean is substantially larger, 0.31 $M_\odot$, with a narrower GSD of 1.7.

Considering the linear momenta and kinetic energies of these objects can provide additional insight. We gathered the expansion velocities from systematic works such as Weinberger (1989). These seem to follow a similar trend to ionised+molecular mass, with values somewhat larger in DD systems than in SD ones. The resulting linear momenta have substantially different geometric means of 6.3×10^{38} g cm s^{-1} (GSD factor 3.5) and 2.2×10^{39} g cm s^{-1} (GSD factor 2.3), for SD and DD systems respectively. The kinetic energies differ in a more pronounced way, with SD systems having a geometric mean of 8.1×10^{44} erg (GSD factor 3.7), whereas DD systems show a much larger 3.9×10^{45} erg (GSD factor 4.2) for DD ones.

https://doi.org/10.1017/S1743921322000205 Published online by Cambridge University Press

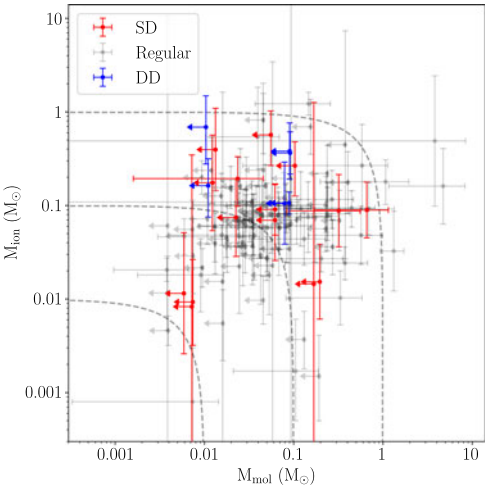

Figure 1. Ionised vs. molecular mass of our post-CE PNe sample and the comparison 'regular' PNe sample. The further to the top and to the right a nebula is, the more massive it is. Dashed lines represent 'isomasses', indicating equal ionised+molecular mass; if neutral atomic mass is neglected, individual nebulae run along these lines as their gas content is progressively ionised.

3.4. *Comparison with regular PNe*

We can put these results in the context of the general population of PNe. Are post-CE PNe more or less massive on average than the general population of PNe? The answer to this question may have strong implications for theories of CE interaction and ejection.

We therefore reviewed the literature in order to derive the ionised and molecular masses of an additional sample of 97 'regular' PNe (not known to arise from binary systems). All of them have dereddened Hα flux and diameters obtained in a systematic way by Frew *et al.* (2016), as well as available ^{12}CO observations and precise distance determinations (either accurate GAIA eDR3 determinations, or being listed as a 'distance calibrator' by Frew *et al.* (2016)). Note that this sample is not limited by volume and is not exempt from selection biases, although the effect of those biases, once filtered by the inclusion criteria, is unclear and difficult to predict. In any case, we stress the intrinsic limitation of the comparison provided in this section, which should be taken with a pinch of salt for the the time being.

The resulting ionised+molecular masses (or their upper limits) of the 'regular' PNe are displayed in Figure 1 along with the results for the SD and DD post-CE PNe analysed in section 3.3. The geometric mean of the mass is the same as that for SD systems, 0.15 $M_\odot$, with a geometric standard deviation (GSD) factor of 3.1. An analysis including the expansion velocities suggests that the characteristic linear momenta of the SD and regular sample are also very similar, although the slightly higher expansion velocities shown by post-CE systems make the kinetic energies of SD post-CE PNe somewhat higher than those of regular PNe. DD systems, on the other hand, show substantially more massive and faster expanding nebulae (larger linear momenta and kinetic energy) than either SD systems and 'regular' PNe.

4. Discussion and conclusions

Our results suggest post-CE PNe hosting SD systems are, on average, neither more nor less massive than regular PNe, whereas post-CE PNe from DD systems are considerably more massive than both groups. This discrepancy is larger when considering the linear

https://doi.org/10.1017/S1743921322000205 Published online by Cambridge University Press

momentum and kinetic energy of these nebulae. In other words, DD systems seem more capable of unbinding and accelerating a larger amount of material than SD systems.

Furthermore, our work suggests a profound mismatch between observations and modelling. On the one hand, models of CE ejection tend to fail to unbind the whole AGB envelope. On the other hand, the observed ionised+molecular mass of these systems seem substantially lower than the expected mass of the AGB envelope at the time of CE occurence, especially in the case of SD systems. In order to quantitatively account for this discrepancy, at least on a first order approximation, we attempted the reconstruction of the CE of two SD systems, Abell 63 and Hen 2-155, and two DD systems, Fg 1 and Hen 2-428. Following the methodology given in Iaconi & De Marco (2019); De Marco (2011), we derived the percentage of the AGB envelope mass that the observed nebula accounts for, as well as the percentage of the orbital shrinking energy budget actually spent on unbinding and accelerating the observed nebula. We find that the mass of the two SD nebulae are ∼1% and ∼22% of their respective AGB envelopes, while for the two DD systems the corresponding figures are ∼64% and ∼61%. Given the large uncertainties, this suggests that DD systems could be unbinding the whole AGB envelope, whereas in the case of SD systems it is hard to reconcile the idea that the observed nebulae is actually the AGB envelope at the time of CE. Examining the energy budget also procures a surprising conclusion: the four analysed systems seem to have spent only between ∼1% and ∼11% of their available orbital shrinking energy budget in unbinding and accelerating their nebulae.

This leads to some uncomfortable questions: If the primary star is of similar mass to normal post-AGB stars, and thus the mass of the nebula amounts to just a tiny fraction of the star's envelope, then where is the rest of the envelope? Why are we unable to detect it somewhere in the vicinity of the star?

References

Balick. B., & Frank, A. 2002, *ARAA*, 40, 439
Chamandy, L., et al. 2020 *MNRAS*, 495, 4028
Corradi, R. L. M., et al. 2015, *ApJ*, 803, 99
De Marco, O. 2011, *MNRAS*, 411, 2277
Decin, L., et al. 2020, *Science*, 369, 1497
Frew, D. J., & Parker, Q. A. 2007, *Proceedings of the APN IV conference*, 475
Frew, D. J., Parker, Q. A., & Bojičić, I. S. 2016, *MNRAS*, 455, 1459
Gaia Collaboration, et al. 2020, *A&A*, 649, 1
Guerrero, M. A., & Miranda, L. F. 2012, *A&A*, 539, 47
Guzman-Ramirez, L. et al. 2018, *A&A*, 618, 91
Huggins, P. J., & Healy, A. P. 1989, *ApJ*, 346, 201
Huggins, P. J., Bachiller, R., Cox, P., & Forveille, T. 1996 *A&A*, 315, 284
Huggins, P. J., Bachiller, R., Planesas, P., Forveille, T., & Cox, P. 2005, *APJS*, 160, 272
Iaconi, R., & De Marco, O. 2019, *MNRAS*, 450, 2550
Ivanova, N. 2018, *ApJL*, 858, 24
Jones, D., & Boffin, H. M. J. 2017, *Nature Astronomy*, 1, 117
Jones, D. 2020, *Reviews in Frontiers of Modern Astrophysics; From Space Debris to Cosmology* (Springer), p. 123
Ohlmann, S. T., Röpke, F. K., Pakmor, R., Springel, V. 2016 *ApJL*, 816, 90
Paczynski, B. 1976, *Proceedings of the IAU Symposium 73*, 75.
Ricker, P. M., & Taam, R. E. 2012, *ApJ*, 746, 74
Santander-García, M., Jones, D., Alcolea, J., Bujarrabal, V., & Wesson, R. 2021, *A&A*, 658, 17
Weinberger, R. 1989, *A&AS*, 78, 301

https://doi.org/10.1017/S1743921322000205 Published online by Cambridge University Press